Published in final edited form as:

Nature. 2024 April ; 628(8006): 47–56. doi:10.1038/s41586-024-07198-2.

Bridging structural and cell biology with cryo-EM

Eva Nogales[1,2,3], **Julia Mahamid**[4,5]

[1]Molecular and Cell Biology Department and Institute for Quantitative Biomedicine, University of California, Berkeley

[2]Molecular Biophysics and Integrated Bioimaging, Lawrence Berkeley

[3]Howard Hughes Medical Institute, Berkeley CA 94720, USA

[4]Structural and Computational Biology Unit, European Molecular Biology Laboratory (EMBL), 69117 Heidelberg, Germany

[5]Cell Biology and Biophysics Unit, EMBL, 69117 Heidelberg, Germany

Preface

Most life scientists would agree that a mechanistic understanding of cellular processes requires structural knowledge of the macromolecules involved. As the primordial example, deciphering the double helical nature of DNA revealed essential aspects of how genetic information is stored, copied and repaired. Yet, reductionist in nature, structural biology requires purification of large amounts of macromolecules, often trimmed off larger functional units. The advent of cryo-EM greatly facilitated the study of large, functional complexes, and generally of samples that are hard to express, purify and/or crystallize. Nevertheless, cryo-EM still requires purification and thus visualization out of the *in situ* context in which macromolecules operate and coexist. On the other hand, cell biologists have been imaging cells by a number of fast-evolving techniques that keep expanding their spatial and temporal reach, but always far from the resolution at which chemistry can be understood. Thus, structural and cell biology provide complementary, yet unconnected visions of the inner workings of cells. Here we discuss how the interplay between cryo-EM and cryo-ET, as a connecting bridge to visualize macromolecules *in situ*, holds great promise to create ever more comprehensive structural depictions of macromolecules as they interact in complex mixtures, or, ultimately, inside the cell itself.

A structural biologist's dream

Imagine you could magically shrink, like in the movie "A Fantastic Voyage", into the realm of the nanometer world, and that you could see, with your own eyes, the intricate molecular jungle filling up our cells (physical laws be darned!). For those of us who have trust in the "seeing is believing" paradigm when it comes to molecular mechanisms, this is probably not an unusual dream. For decades, structural biologists have used a poor-man's approach to such dreams by painstakingly purifying their biological macromolecule of interest out of its cellular context and employing the tools of the trade to generate atomic models, if lucky, in several functional states, so as to infer the chemical and physical rules that govern their functioning. This reductionist approach has populated the protein data bank (PDB) [1] at an ever-increasing rate and has allowed us to generate a physical framework that integrates

biochemical and biophysical data, that maps human mutations, that predicts or helps to improve small molecule binding for therapeutic purposes, or, in the momentous recent age, to map viral mutations that escape our antibodies or could weaken the effectiveness of our vaccines. Valuable as our visualization of macromolecular structure is out of the context of the cell, it is clear that the tunnel vision it provides is only a small part of a bigger, more complex story that ultimately has to include the molecular sociology [2] that necessarily governs cellular function, as cell biologists will be ready to tell you. The closest thing to our dream so far has been to contemplate the fabulous and aesthetically pleasing imagery of cellular landscapes that the talented David Goodsell has created using the PDB, other available data, and an incredible taste for color [3] (Figure 1).

Shrinking fantasies and beautiful drawings aside, macromolecules can be “seen” both inside and outside of our cells, just not with our eyes, not with light, and not without some compromise. This article deals with the use of electrons and the study of frozen-in-time molecules and cells by the sister methodologies of single particle cryogenic electron microscopy (from now on referred to as cryo-EM) and cryogenic electron tomography (cryo-ET) (see Box 1). It will not detail the principles behind such techniques or be a comprehensive summary of exciting new structures and cellular landscapes, for which we direct the readers to some excellent recent reviews [4–8]. Instead, it is an attempt to look into the present and towards the future of how different combinations of electron microscopy methods that visualize cryogenically preserved biological samples with different levels of complexity can bring us closer to our ultimate dream of understanding, mechanistically, how macromolecules operate inside our cells to generate the adaptive and responsive complexity of the biological world.

Cryo-EM, a technique born several decades ago but that has gained center stage among structural biology methods in the last one [9], has several advantages with respect to X-ray crystallography or NMR, including the fact that, typically, much less sample material is needed and that there is no upper limit in the size of the macromolecule under study. These properties have made cryo-EM the method of choice to study many “omes”, that is, the (reasonably) stable complex molecular machinery that govern, among others, the central dogma (e.g. DNA replication [10] and repair [11], transcription [12], splicing [13], translation [14], protein folding [15], protein degradation [16], etc.), to obtain the structure of integral membrane proteins such as ion channels [17], viral proteins [18], signaling complexes [19], or photosynthesis complexes [20], or to visualize biological polymers at ever increasing resolution [21,22]. Within this last decade, methodological improvements in cryo-EM have increased its throughput, applicability, and resolution (now with demonstrated true atomic resolution for both simple test samples [23] and large complex assemblies [14]), and with them increased the biological insight that this method has been able to provide. In parallel, cryo-ET, which promises *in situ* visualization of all those macromolecules as they interact with each other in the complex cellular milieu, has started to overcome some of the technical hurdles that are inherent to the study of cells [4,24]: the need to generate thin samples (via mechanical cryo-sectioning [25–27] or now more often by focused ion beam (FIB) milling [28–31]), the compromised quality of images of tilted samples while maintaining a tolerable electron dose, the limited resolution in the subsequent tomographic reconstructions, or the interpretability of those cellular volumes permitted by the low signal-to-noise ratio compounded by the dense and

complex nature of the cell [32]. If you are interested in a particular biological process, you are likely to consider the use of both methods. In fact, the two sister techniques can feed each other to provide biological insight that is more than the sum of the parts. For example, the high-resolution structures of large macromolecular complexes, polymers or membrane proteins, as obtained by cryo-EM of purified complexes, can help to find those structures in the cell when seen in cryo-tomograms, or subtomogram averages of a certain complex as obtained from analysis of cryo-ET data can be interpreted by comparison with those structures of the complex obtained under controlled *in vitro* conditions. There are clearly multiple experimental paths across both techniques and here we would like to propose some that can be used to gain mechanistic information in the pursuit of a certain biological process. These are very likely not the only ones possible.

Technical advances in cryo-EM and cryo-ET

A number of technological breakthroughs have transformed the capabilities of both cryo-EM and cryo-ET over the last decade. Arguably, the most dramatic effect on both methods has come from the development and commercialization of better detector technology. The so-called direct electron detectors (DED) have dramatically improved the contrast and resolution of the images [33]. Improving quantum efficiency and allowing for the correction of beam-induced motion (through alignment of video frames permitted by the fast readout of the cameras) [34] have both contributed to the highly improved performance of DEDs with respect to film. Automation of data collection and quality of the optical system of modern microscopes have also contributed to the quality and quantity of the images obtained and have led both to the general applicability of cryo-EM and to its much-improved resolution. When it comes to cryo-ET of intact cells, where the major bottleneck for decades had been thinning of the sample to electron transparency, the adaptation of focused ion beam milling, commonly employed in the material sciences, to cryogenic samples finally provided an essential and routine solution that significantly minimizes perturbation to the sample [28–31,35–37] in comparison to traditional cryo-sectioning [25].

Perhaps as important as the hardware advances are the development of new software platforms that have taken advantage of the improved images and of Bayesian approaches to separate conformational/compositional states of the sample and discard contaminating or damaged particles that before contributed negatively to cryo-EM reconstructions [38–40]. Schemes of 2D and 3D classification are now nested within the pipeline of image analysis, in ways that are still often sample and user specific, and that have allowed the improvement of resolution, and that often also describe, to different extents, the conformational landscape of the molecule under study. While streamlined software solutions are now more developed for the analysis of single particle cryo-EM data, processing of cryo-ET data faces similar challenges and is handled through analogous, though more involved and somewhat less effective, pipelines [41–43]. Furthermore, inherent to visualizing functional molecules within the cellular context involves capturing a potentially wide variety of interaction partners and/or conformations, which will require powerful software to untangle such complexity during the generation and analysis of subtomogram averages. New machine-learning methodologies are also addressing the challenge of describing continuous conformational changes in macromolecules [40,44,45] and thus have the potential to provide novel insights

into the complex conformational landscapes that are often at the heart of macromolecular function.

Sample complexity in cryo-EM and cryo-ET

The nature of the sample under study will be what ultimately determines which imaging technique to use (Figure 2). In cryo-EM, the assumption is that the object being studied is simple in terms of compositional and conformational variation: for example, purified ribosomes (although likely in multiple states) would typically be the subject of cryo-EM. On the other hand, higher-order assemblies of ribosomes in polysomes present in a cell will be imaged via cryo-ET. This reasoning takes us back to the initial consideration of cryo-EM as a more "classical" reductionist, structural biology method, while cryo-ET holds the promise of imaging the cellular content in its somewhat chaotic and complex beauty. However, there is almost a continuum in the nature of the complexity of a sample; this spectrum necessarily challenges simple distinctions and blurs the boundaries of when one method can be used versus the other. What follows is a proposal of different levels of sample complexity and the role that cryo-EM and cryo-ET can play in their structural characterization.

- Traditional sample purification:

The pipeline of sample preparation for cryo-EM often parallels that used for traditional structure determination, say, by X-ray crystallography: overexpression of the macromolecule or complex in a heterologous system followed by strict purification aiming for a single biochemical species. However, because there is no need to obtain crystals, and because of the nature of electron scattering, typically much less sample is required in the case of cryo-EM. Thus, biological samples traditionally hard to overexpress in large amounts, such as integral membrane proteins [46,47] (which can even be studied embedded in lipids [48]) or large complexes of many components [49–51], are more accessible by cryo-EM. But it is even more important to mention that the light requirements in terms of sample concentration for cryo-EM mean that it is possible to rely on endogenously purified material for structural studies, even when the complex pursued is present in low abundance in cells [52]. A general strategy could be to CRISPR-engineer a cell line in which one of the subunits of a complex of interest has been chromosomally tagged for affinity purification [53,54]. The advantage of this method is that the purification scheme can be relatively simple and preserve the integrity of assemblies, so as to guarantee a close resemblance to the state of the complex in the cell, including subunit composition and post-translational modifications. Samples can then be concentrated for imaging via different forms of "affinity grids" [55–57]. Although this "milder" purification scheme may lead to samples of increased biochemical complexity (which could be defined via mass spectrometry), it is reasonable to expect that it will still be constrained to a finite number of molecular entities that can be dealt with using single particle cryo-EM principles. Furthermore, the arrival at a single species may not be easily achievable, and in some cases, not even desired. In cases where a limited number of macromolecules (e.g. 2–5) co-purify in the chosen final step (e.g. membrane fractions from an organelle that are separated in a sucrose gradient [58]), it has proven possible to deal with the different species simultaneously during cryo-EM data processing. The system needs to be still simple enough to have a defined part list that would help with the processing by guiding the number

of species expected during classification and reconstruction. On the other hand, purified samples that are nevertheless pleomorphic, like enveloped viruses [59] or ribonuclear particles (RNPs) that have an ill-defined stoichiometry [60], are typically considered more suitable to cryo-ET characterization.

- Complex reconstitutions:

When the system reconstituted from purified components gains in complexity due to the number of molecular parts and/or unique arrangements of those parts (e.g., multiple interactors bound to a cytoskeletal polymer [61], or coat protein-membrane assemblies [62]) it may be necessary to use non-trivial, tailored single particle schemes to deal with this complexity, or cryo-ET followed by subtomogram averaging and classification. Collecting both modalities of data and analyzing those datasets in parallel for systematic comparison of the resulting structures and interpretation may prove to be the most robust way to gain functional conclusions in some of the most complex reconstituted systems.

- Crude purifications:

Interestingly, it has become possible to relax the “extraction” process to deal with only partially purified material (e.g. size exclusion fractions of a cell lysate) and pursue the simultaneous cryo-EM reconstruction of several macromolecules from a single grid/dataset of a highly complex mixture. In this way, a chromatographic method is used to separate components into “bins” based on size or charge, and different fractions are analyzed in consecutive cryo-EM studies. Examples include human cell extracts [63], eukaryotic thermophile cell extracts [64], malaria parasite cell lysates [65], and detergent-solubilized membrane pellets from bacteria [66]. Such approaches are faced with the challenge of grouping the single particle cryo-EM images according to different structures when there is no or little pre-existing knowledge of such structures, or even of how many should be expected to be present (here, mass spectrometry can provide some useful information). As of today, the process cannot be done reliably without some human intervention in the early stages of generating initial models, and so far, its implementation has concentrated on the most abundant and/or featureful molecules (large, symmetric). In this context, a more objective way of generating initial models to seed the image analysis process, with the potential to pursue the structure determination in a more systematic way, should be considered. One possibility would be to obtain cryo-ET data from the same sample grid to generate initial models. Whether the “raw” volumes would be sufficient or some subtomogram classification, not without its own limitations when dealing with highly heterogenous samples, need to be carried out may depend on the nature of the molecules and the quality of the tomograms. Imaging schemes that maximize the signal, such as phase plates [67,68], may be beneficial to simplify the process of generating initial models from cryo-ET that can be used for cryo-EM analysis of complex mixtures.

- Cell fractions:

A bootstrapping step moving from purified systems, of any complexity, to looking inside a cell, is the visualization of cellular fractions. Extracts and cell fractions have been broadly used for decades to elucidate cellular pathways. In the context of cryo-EM imaging in the transmission electron microscope, the advantages of the extract over working with

intact cells include overcoming the bottleneck of generating thin cellular sections, and the opportunity to manipulate the extract to either remove components (e.g. by immuno-depletion) or by adding them, via overexpression in cell culture systems or by exogenous addition [69]. In the latter case, added key components could be fluorescently labeled so that they can be followed by correlative light and electron microscope methods, or even labeled with an electron-dense marker for direct identification in cryo-EM, without the need of generating a more complex *in vivo* labeling scheme. The benefits of the extract with respect to a complex reconstitution is that it does not involve purification of components, which in some cases faces technical bottlenecks. It also provides a more physiological environment where functionally relevant partners that may not yet be known are present, and where the "crowdedness" of the cellular milieu can be maintained if desired. More recently, methods have emerged combining microfluidic single-cell extraction with single-particle analysis by EM to characterize protein complexes from individual *Caenorhabditis elegans* embryos [70]. On the other hand, working with cell extracts is a compromise where interpretation may be just as difficult as in an *in situ* study, yet where the true cellular context has been lost. In general, it is likely that these systems will need to be studied by cryo-ET.

- Working with intact cells:

In many cases, the biological question being addressed will require looking directly into the cell or tissue. If a molecular interpretation of the cellular landscape is desired, the cell or tissue will first have to be vitrified. Depending on the original thickness of the biological object, traditional plunge freezing can be used (e.g. for single cells) [26] or high-pressure freezing [71] may be required (e.g. for multicellular or tissue samples). Regardless of the vitrification method, the ideal sample for analysis with a reasonable signal-to-noise ratio requires a sample thickness of less than 0.3 μm (and ideally half of that!). This can be accomplished via cryo-sectioning, or, more commonly these days, via focused ion beam (FIB) milling [28,29], typically coupled to scanning electron microscopy (SEM) to monitor the process and visualize the resulting lamella. These thin sections or lamellae will be the ones introduced into the transmission electron microscope and imaged, most commonly, via cryo-ET. Until recently, cellular thinning and high-quality cryo-ET data acquisition on FIB lamellae were accessible to just a few experts. But the increasing availability of commercial, out-of-the-box hardware solutions [72], knowledge transfer and standardization of sample preparation [31,73,74], innovation in integrated instrumentation (e.g. inclusion of a light microscope in the FIB chamber [75–78] to minimize cumbersome sample transfers between microscopes), and automation both in FIB preparations [79,80] and large-scale cryo-ET imaging [81–83], are gradually making these methods more widely available across the life sciences and to non-expert communities through service provisions in large national centers.

Extracting information in complex samples

What kind of information can be obtained when the complexity or nature of the sample requires cryo-ET? Cryo-tomograms are often interpreted after some denoising [84–86], segmentation, and/or localization of the most obvious elements, such as membranes, cytoskeletal polymers and large macromolecular assemblies like ribosomes. The identification of the structures of interest in the cellular milieu (or in complex mixtures/

cellular extracts) can be performed by computational pattern recognition using, for example, templates from high resolution structures and matching them with the tomograms (as discussed below) employing either traditional cross correlation [87], supervised deep-learning [88,89] or by unsupervised algorithms [90] (which still require substantial developments and validation). There are two additional alternative approaches for particle identification based on tagging the component of interest. The first involves the use of correlated light and electron microscopy of fluorescently tagged complexes [91–94], for which methodologies are being developed to overcome the diffraction limit of light (i.e. super-resolution approaches) in order to achieve registration precision on the scale of ~10 nm in cryogenically preserved samples [95–97]. The second entails the use of molecular tags that can directly pinpoint the location of the complex of interest in cryo-tomograms. Current applications involve either electron-dense particles that produce high contrast in the electron microscope [98] or self-assembling particles with distinct shapes that can be identified using template matching or machine learning algorithms [99,100].

Bona fide structural understanding will often require analyses that go beyond segmentation and localization. Similar to single particle cryo-EM, obtaining a molecular structure from cryo-ET requires averaging and classifying multiple copies of similar entities, especially when attempting to disentangle variability with a higher level of detail and resolution. Therefore, populations of conformations with low abundance can be easily missed. While in single particle cryo-EM this is typically addressed by enriching the particular entity or state in the specimen, acquiring large numbers of particle images, and employing classification schemes, for cryo-ET a brute force approach for higher throughput data collection is typically the only way to achieve this. Cryo-ET is limited in throughput compared to cryo-EM, although recent developments [82,101] have dramatically improved the speed at which tomograms can be collected. On the other hand, despite the power of FIB-SEM to produce thin cellular lamellae, this methodology is still not perfect, and samples are not entirely undamaged by the thinning process [102,103]. Contrast, too, remains a limitation in cryo-ET. Thicker and more complex samples results in necessarily reduced contrast compared to that obtained from purified cryo-EM samples. Lastly, non-trivial sample preparation and analysis pipelines still require substantial expertise and painstakingly acquired knowledge of experimental details. Nevertheless, combinations of the technical advances mentioned above will soon lead to the generation of thousands of tomograms for each biological process or object of interest. As they stand, current applications of state-of-the-art cryo-ET, in its different flavors and in combination with correlative methods, are already providing unprecedented insights into complex cell biology, even when they do not produce high resolution subtomogram averages from macromolecules imaged in situ. A few breath-taking examples include bacterial cell biology of phage infection [104], the exceptionally complex regulation of molecular transport in specialized cellular sub-compartments [105], and inter-organelle membrane contact sites in eukaryotes [106] (Figure 3). These examples represent only a glimpse into the outstanding impact cryo-ET, when integrated with structural modeling, will likely have in bridging structural and cell biology.

Interplay between cryo-EM and cryo-ET

Because the resolution of structures that can be generated by cryo-ET is often lower than that of cryo-EM, but the former provides a more physiological context all the way to the native cell or tissue, the two approaches are naturally complimentary. As indicated above, cryo-EM is somehow limited by the reductionist nature inherent to the process of purification, although it can readily deal with large assemblies containing many subunits and therefore study fully biochemically functional complexes. The more transient interactions of such "stable" complexes with regulatory factors can also be studied in this way. These "supramolecular" assemblies are very likely to resemble those in mild purifications, extracts, or inside the cell. Thus, cryo-EM structures are ideal to interpret lower-resolution cryo-ET maps derived from more complex systems (e.g. extracts, cells). Additional complementary structural methods, both experimental and computational (i.e. predictions [107,108]) can also be used. While integrative modeling can be used to combine predicted structures of individual components with additional information, such as cross-linking mass spectrometry [109,110], large complexes are not yet in the realm of what can be systematically predicted. Therefore, the larger molecular sizes studied by cryo-EM, often providing multiple functional states, gives it an advantage, and structures generated by cryo-EM can be readily used to interpret the complex cryo-ET reconstructions.

One obvious way in which cryo-EM and cryo-ET can be combined concerns the use of cryo-EM structures as templates [87] to search tomographic volumes and identify the position of the corresponding molecule in the cellular context. The low signal in tomograms has so far restricted this approach to relatively large complexes, such as ribosomes or proteosomes, and this method has yet to be broadly successfully applied even to particles in the hundreds of kDa range. An alternative to 3D template matching on tomographic volumes is to perform 2D template matching in single, high-resolution images of cellular slices [111,112] (Figure 4). Here, the identification of the molecule of interest relies on high-resolution features in the image, and the accuracy in finding a match requires high similarity between the template and the biological object in the micrograph. While the shortcoming is that the precise high-resolution structure may not be available, the upside is that the method should be able to discriminate even different conformational states of each instance of the object (without resorting to averaging and classification) if such structures are available in the PDB or can be computationally generated (say, through molecular dynamics simulations). On the other hand, additional co-factors that interact with the complex in the native cellular context may be potentially recovered using alignment and averaging strategies analogous to single particle cryo-EM [113]. While algorithms are still being developed to carefully address the expected strong template bias, the mere emergence of such extra densities in the analysis (when they did not exist in the template) provides strong evidence that new structures could be obtained using 2D template matching, and promise an exciting opportunity to complement cryo-ET approaches in obtaining high resolution structures *in situ*. On the other hand, 2D template matching, by concentrating on specific molecular targets, does not provide a more complete view of the subcellular environment (e.g. a volumetric description of membranes, the cytoskeleton or other unknown molecular assemblies).

To date, both 3D and 2D template matching have been demonstrated only for a handful of large complexes and both remain computationally expensive. How far each of these methods can go in identifying smaller complexes based on experimentally or computationally generated structures is not yet known. Each method is likely to improve in the future, both with better images obtained with new phase plate-based instruments and/or better detectors, and with the improvement of processing algorithms. While the choice of one versus the other may depend on the biological question being asked, one option to explore would be to obtain both cryo-EM and cryo-ET and carry out both 2D and 3D template matching on the same sample region. Both types of template matching could be done in parallel, and the results compared [111]. When used sequentially, a lower-resolution tomogram (in this case, somewhat reduced in quality by the ~20 e^{-}/A^{2} invested in a first 2D high-resolution projection) would visualize the 3D environment that gives context to the analysis by 2D template matching. Optimization of both with the right type of test cases would allow objective validation, perhaps using more simplified systems, before we are able to move fully into the systematic analysis of complex cellular sociology that is ultimately the target.

Beyond cryo-EM and cryo-ET

The major advantage of studying intact cells by cryo-ET is its potential to capture the full set of macromolecules and their interaction partners in a context-dependent manner. However, the use of thin cellular slices (~200 nm) and the restricted field of view associated with the angstrom-range pixel sizes, both required to achieve high-resolution imaging, dramatically limit the region being visualized out of the full cell or multicellular specimen. Cryo-ET studies are often complemented by correlative imaging modalities, most commonly fluorescence microscopy, sometimes with super-resolution methods, to provide essential knowledge on the location and identity of a subcellular structure or molecular assembly, both to guide the FIB milling process and the subsequent cryo-ET data collection and interpretation. But fluorescence-based imaging suffers from the limitation of visualizing a selected number of tagged molecules or organelles. Room temperature FIB-SEM [114,115] or SEM block face [116] volume imaging, and cryogenic X-ray imaging [117] are increasingly used to generate volumetric data on cellular ultrastructure at resolutions spanning 10–50 nm. These imaging methods reveal the intricate connectivity between cellular organelles, their abundance and distributions across entire cells, even within complex multicellular tissues or entire organisms. Ultimately, to connect molecular-level structures obtained by cryo-EM/ET to function at the cellular and organismal level will require further developments in large-volume imaging methods of frozen hydrated samples, which could then be followed by FIB milling and/or extraction of specific sections [35,37] for subsequent cryo-ET. Such methodology is just starting to emerge and will mature over the coming years. Finally, with cryo-ET methods fast evolving on multiple fronts towards higher throughput, they could be complemented by the integration of multi-omics single-cell data (e.g., high-throughput and quantitative light microscopy, transcriptomics, metabolomics, and proteomics) to reveal the beautiful variability and stochasticity of biological processes across cells. When combined with high resolution structures from cryo-EM of purified macromolecular complexes, a new mechanistic understanding of cellular processes and their regulation is sure to emerge.

The structural databases (see Box 2 on a perspective of past and future structure data bases) have contributed to the emergence of transformative protein structure prediction, which has taken structural biology by storm. While the world of structure prediction had progressed at a steady but frustrating pace for years, what AI methods like AlphaFold [108] or RosettaFold [107] can now do has elevated structure prediction to a totally new level. As the reach of these methods expands to predict complexes that include multiple protein chains, many even wonder what the future of experimental structural biology is. Obviously, AI protein structure prediction can be a strong ally that augments the reach and speeds up structural biology. Predictions may guide selection of samples to study or generate expectations concerning well versus poorly structured regions. Most importantly in an EM study, once a cryo-EM/ET density is available, predictions can speed up atomic model building by providing initial structures of all potential or actual parts of the complex, which can then be refined more carefully into the experimental density map. For *in situ* studies, predictions can be used to generate templates for 2D and 3D template matching, a principle that will become more applicable as the tomograms quality and template matching schemes allow detection of smaller entities and/or predictions can be applied to large complexes with many subunits. What is clear is that today bootstrapped paths from AI-based predictions to cryo-EM experimental structures of large assemblies and to the interpretation of intracellular landscapes captured by cryo-ET in terms of molecular structure are already a reality.

Acknowledgments

We are grateful to our group members and many colleagues for fruitful discussions. We thank those who provided figures for reproduction in this review, and we apologize to those whose outstanding work we have not been able to cite due to the limited number of references. E.N. acknowledges support from the national Institutes of Health (R35GM127018). She is a Howard Hughes Medical Institute Investigator. J.M. acknowledges valuable assistance from Joseph Dobbs, and support from the EMBL, a European Research Council starting grant (3DCellPhase¯760067) and a Chan-Zuckerberg Initiative grant for Visual Proteomics.

References

1. Berman H, Henrick K & Nakamura H Announcing the worldwide Protein Data Bank. Nat Struct Biol 10, 980 (2003). 10.1038/nsb1203-980 [PubMed: 14634627]

*2. Robinson CV, Sali A & Baumeister W The molecular sociology of the cell. Nature 450, 973–982 (2007). 10.1038/nature06523 [PubMed: 18075576] This seminal review coined the term “molecular sociology” and set the scence for future in situ structural biology that combine cryo-ET with proteomics via integrative modeling.

3. Span EA et al. Protein structure in context: the molecular landscape of angiogenesis. Biochem Mol Biol Educ 41, 213–223 (2013). 10.1002/bmb.20706 [PubMed: 23868376]

4. Bäuerlein FJB & Baumeister W Towards Visual Proteomics at High Resolution. J. Mol. Biol 433, 167187 (2021). 10.1016/j.jmb.2021.167187 [PubMed: 34384780]

5. Berger C et al. Cryo-electron tomography on focused ion beam lamellae transforms structural cell biology. Nature Methods 20, 499–511 (2023). 10.1038/s41592-023-01783-5 [PubMed: 36914814]

6. Chua EYD et al. Better, Faster, Cheaper: Recent Advances in Cryo-Electron Microscopy. Annu. Rev. Biochem 91, 1–32 (2022). 10.1146/annurev-biochem-032620-110705 [PubMed: 35320683]

7. Wu M & Lander GC Present and Emerging Methodologies in Cryo-EM Single-Particle Analysis. Biophys. J 119, 1281–1289 (2020). 10.1016/j.bpj.2020.08.027 [PubMed: 32919493]

8. Young LN & Villa E Bringing Structure to Cell Biology with Cryo-Electron Tomography. Annual Review of Biophysics 52, 573–595 (2023). 10.1146/annurev-biophys-111622-091327

9. Kühlbrandt W The Resolution Revolution. Science 343, 1443–1444 (2014). 10.1126/science.1251652 [PubMed: 24675944]

10. Lewis JS et al. Mechanism of replication origin melting nucleated by CMG helicase assembly. Nature 606, 1007–1014 (2022). 10.1038/s41586-022-04829-4 [PubMed: 35705812]

11. Chen S et al. Structural basis of long-range to short-range synaptic transition in NHEJ. Nature 593, 294–298 (2021). 10.1038/s41586-021-03458-7 [PubMed: 33854234]

*12. Chen X et al. Structures of +1 nucleosome-bound PIC-Mediator complex. Science (New York, N.Y.) 378, 62–68 (2022). 10.1126/science.abn8131 [PubMed: 36201575] This study is an inspiring example of the large size and complexity of reconstitution systems amenable for cryo-EM study. It visualized an assembly of eight transcription complexes, some over 1 MDa in size, on chromatin.

13. Tholen J, Razew M, Weis F & Galej WP Structural basis of branch site recognition by the human spliceosome. Science (New York, N.Y.) 375, 50–57 (2022). 10.1126/science.abm4245 [PubMed: 34822310]

14. Fromm SA et al. The translating bacterial ribosome at 1.55 Å resolution generated by cryo-EM imaging services. Nature communications 14, 1095 (2023). 10.1038/s41467-023-36742-3

15. Gestaut D et al. Structural visualization of the tubulin folding pathway directed by human chaperonin TRiC/CCT. Cell 185, 4770–4787.e4720 (2022). 10.1016/j.cell.2022.11.014 [PubMed: 36493755]

16. Bashore C et al. Targeted degradation via direct 26S proteasome recruitment. Nat Chem Biol 19, 55–63 (2023). 10.1038/s41589-022-01218-w [PubMed: 36577875]

17. Zhang K, Julius D & Cheng Y Structural snapshots of TRPV1 reveal mechanism of polymodal functionality. Cell 184, 5138–5150 e5112 (2021). 10.1016/j.cell.2021.08.012 [PubMed: 34496225]

18. Kern DM et al. Cryo-EM structure of SARS-CoV-2 ORF3a in lipid nanodiscs. Nature Structural & Molecular Biology 28, 573–582 (2021). 10.1038/s41594-021-00619-0

19. Lin X et al. Cryo-EM structures of orphan GPR21 signaling complexes. Nature communications 14, 216 (2023). 10.1038/s41467-023-35882-w

20. Domínguez-Martín MA et al. Structures of a phycobilisome in light-harvesting and photoprotected states. Nature 609, 835–845 (2022). 10.1038/s41586-022-05156-4 [PubMed: 36045294]

21. Oosterheert W, Klink BU, Belyy A, Pospich S & Raunser S Structural basis of actin filament assembly and aging. Nature 611, 374–379 (2022). 10.1038/s41586-022-05241-8 [PubMed: 36289337]

22. Reynolds MJ, Hachicho C, Carl AG, Gong R & Alushin GM Bending forces and nucleotide state jointly regulate F-actin structure. Nature 611, 380–386 (2022). 10.1038/s41586-022-05366-w [PubMed: 36289330]

23. Nakane T et al. Single-particle cryo-EM at atomic resolution. Nature 587, 152–156 (2020). 10.1038/s41586-020-2829-0 [PubMed: 33087931]

*24. Beck M & Baumeister W Cryo-Electron Tomography: Can it Reveal the Molecular Sociology of Cells in Atomic Detail? Trends Cell Biol 26, 825–837 (2016). 10.1016/j.tcb.2016.08.006 [PubMed: 27671779] A landmark review that discusses how recent technological breakthroughs in sample thinning, combined with direct electron deteciton and phase plates hold promise to achieve near-atomic reconstructions by in situ cryo-ET.

25. Al-Amoudi A, Studer D & Dubochet J Cutting artefacts and cutting process in vitreous sections for cryo-electron microscopy. J. Struct. Biol 150, 109–121 (2005). 10.1016/j.jsb.2005.01.003 [PubMed: 15797735]

26. McDowall AW et al. Electron microscopy of frozen hydrated sections of vitreous ice and vitrified biological samples. J. Microsc 131, 1–9 (1983). 10.1111/j.1365-2818.1983.tb04225.x [PubMed: 6350598]

27. Gan L, Ng CT, Chen C & Cai S A collection of yeast cellular electron cryotomography data. Gigascience 8 (2019). 10.1093/gigascience/giz077

28. Marko M, Hsieh C, Schalek R, Frank J & Mannella C Focused-ion-beam thinning of frozen-hydrated biological specimens for cryo-electron microscopy. Nature Methods 4, 215–217 (2007). 10.1038/nmeth1014 [PubMed: 17277781]

29. Rigort A et al. Focused ion beam micromachining of eukaryotic cells for cryoelectron tomography. Proceedings of the National Academy of Sciences 109, 4449–4454 (2012). 10.1073/pnas.1201333109

30. Schaffer M et al. Optimized cryo-focused ion beam sample preparation aimed at in situ structural studies of membrane proteins. J Struct Biol 197, 73–82 (2017). 10.1016/j.jsb.2016.07.010 [PubMed: 27444390]

31. Wagner FR et al. Preparing samples from whole cells using focused-ion-beam milling for cryo-electron tomography. Nature Protocols 15, 2041–2070 (2020). 10.1038/s41596-020-0320-x [PubMed: 32405053]

32. Lucic V, Rigort A & Baumeister W Cryo-electron tomography: the challenge of doing structural biology in situ. J Cell Biol 202, 407–419 (2013). 10.1083/jcb.201304193 [PubMed: 23918936]

33. Faruqi AR & McMullan G Direct imaging detectors for electron microscopy. Nuclear Instruments and Methods in Physics Research Section A: Accelerators, Spectrometers, Detectors and Associated Equipment 878, 180–190 (2018). 10.1016/j.nima.2017.07.037

34. Campbell MG et al. Movies of ice-embedded particles enhance resolution in electron cryo-microscopy. Structure (London, England: 1993) 20, 1823–1828 (2012). 10.1016/j.str.2012.08.026 [PubMed: 23022349]

35. Schaffer M et al. A cryo-FIB lift-out technique enables molecular-resolution cryo-ET within native Caenorhabditis elegans tissue. Nature Methods 16, 757–762 (2019). 10.1038/s41592-019-0497-5 [PubMed: 31363205]

36. Kelley K et al. Waffle Method: A general and flexible approach for improving throughput in FIB-milling. Nature communications 13, 1857 (2022). 10.1038/s41467-022-29501-3

*37. Schiøtz OH et al. Serial Lift-Out: sampling the molecular anatomy of whole organisms. Nat Methods (2023). 10.1038/s41592-023-02113-5 This work presents developments that significantly improve success rates and reproducibility in cryo-FIB micromachining and micromanipulator-assisted lift-out for production of samples suitable for cryo-ET from small multicellular model organisms.

38. Punjani A, Rubinstein JL, Fleet DJ & Brubaker MA cryoSPARC: algorithms for rapid unsupervised cryo-EM structure determination. Nature Methods 14, 290–296 (2017). 10.1038/nmeth.4169 [PubMed: 28165473]

39. Scheres SHW Processing of Structurally Heterogeneous Cryo-EM Data in RELION. Methods Enzymol 579, 125–157 (2016). 10.1016/bs.mie.2016.04.012 [PubMed: 27572726]

40. Zhong ED, Bepler T, Berger B & Davis JH CryoDRGN: reconstruction of heterogeneous cryo-EM structures using neural networks. Nature Methods 18, 176–185 (2021). 10.1038/s41592-020-01049-4 [PubMed: 33542510]

*41. Tegunov D, Xue L, Dienemann C, Cramer P & Mahamid J Multi-particle cryo-EM refinement with M visualizes ribosome-antibiotic complex at 3.5 Å in cells. Nature Methods 18, 186–193 (2021). 10.1038/s41592-020-01054-7 [PubMed: 33542511] This work developed novel algorithms that allowed correction of sample deformation during cryo-ET acquisition to obtain the first near-atomic reconstruction of a macromolecular complex inside cells.

42. Wan W, Khavnekar S, Wagner J, Erdmann P & Baumeister W STOPGAP: A Software Package for Subtomogram Averaging and Refinement. Microscopy and Microanalysis 26, 2516–2516 (2020). 10.1017/S143192762002187X

43. Zivanov J et al. A Bayesian approach to single-particle electron cryo-tomography in RELION-4.0. eLife 11, e83724 (2022). 10.7554/eLife.83724 [PubMed: 36468689]

44. Powell BM & Davis JH Learning structural heterogeneity from cryo-electron sub-tomograms with tomoDRGN. bioRxiv (2023). 10.1101/2023.05.31.542975

45. Rangan R et al. Deep reconstructing generative networks for visualizing dynamic biomolecules inside cells. bioRxiv (2023). 10.1101/2023.08.18.553799

46. Allard CAH et al. Structural basis of sensory receptor evolution in octopus. Nature 616, 373–377 (2023). 10.1038/s41586-023-05822-1 [PubMed: 37045920]

47. Xu W et al. Structural basis for strychnine activation of human bitter taste receptor TAS2R46. Science (New York, N.Y.) 377, 1298–1304 (2022). 10.1126/science.abo1633 [PubMed: 36108005]

48. Yao X, Fan X & Yan N Cryo-EM analysis of a membrane protein embedded in the liposome. Proc. Natl. Acad. Sci. U. S. A 117, 18497–18503 (2020). 10.1073/pnas.2009385117 [PubMed: 32680969]

49. Mühleip A et al. Structural basis of mitochondrial membrane bending by the I–II–III2–IV2 supercomplex. Nature 615, 934–938 (2023). 10.1038/s41586-023-05817-y [PubMed: 36949187]
50. Vallese F et al. Architecture of the human erythrocyte ankyrin-1 complex. Nature Structural & Molecular Biology 29, 706–718 (2022). 10.1038/s41594-022-00792-w
51. Walton T et al. Axonemal structures reveal mechanoregulatory and disease mechanisms. Nature, 1–9 (2023). 10.1038/s41586-023-06140-2
52. Abdella R et al. Structure of the human Mediator-bound transcription preinitiation complex. Science 372, 52–56 (2021). 10.1126/science.abg3074 [PubMed: 33707221]
53. Herbst DA et al. Structure of the human SAGA coactivator complex. Nature Structural & Molecular Biology 28, 989–996 (2021). 10.1038/s41594-021-00682-7
54. Liu H, Li A, Rochaix J-D & Liu Z Architecture of chloroplast TOC–TIC translocon supercomplex. Nature 615, 349–357 (2023). 10.1038/s41586-023-05744-y [PubMed: 36702157]
55. Kelly DF, Abeyrathne PD, Dukovski D & Walz T The Affinity Grid: a pre-fabricated EM grid for monolayer purification. J. Mol. Biol 382, 423–433 (2008). 10.1016/j.jmb.2008.07.023 [PubMed: 18655791]
56. Han B-G et al. Long shelf-life streptavidin support-films suitable for electron microscopy of biological macromolecules. J. Struct. Biol 195, 238–244 (2016). 10.1016/j.jsb.2016.06.009 [PubMed: 27320699]
57. Wang F et al. General and robust covalently linked graphene oxide affinity grids for high-resolution cryo-EM. Proc. Natl. Acad. Sci. U. S. A 117, 24269–24273 (2020). 10.1073/pnas.2009707117 [PubMed: 32913054]
58. Maldonado M, Guo F & Letts JA Atomic structures of respiratory complex III2, complex IV, and supercomplex III2-IV from vascular plants. eLife 10, e62047 (2021). 10.7554/eLife.62047 [PubMed: 33463523]
59. Peukes J et al. The native structure of the assembled matrix protein 1 of influenza A virus. Nature 587, 495–498 (2020). 10.1038/s41586-020-2696-8 [PubMed: 32908308]
*60. Pacheco-Fiallos B et al. mRNA recognition and packaging by the human transcription-export complex. Nature 616, 828–835 (2023). 10.1038/s41586-023-05904-0 [PubMed: 37020021] This study is a beautiful example of the combination of single particle cryo-EM and cryo-ET in the structural chgaracterization of a complex biological assembly.
61. Ferro LS et al. Structural and functional insight into regulation of kinesin-1 by microtubule-associated protein MAP7. Science 375, 326–331 (2022). 10.1126/science.abf6154 [PubMed: 35050657]
62. Hooy RM, Iwamoto Y, Tudorica DA, Ren X & Hurley JH Self-assembly and structure of a clathrin-independent AP-1:Arf1 tubular membrane coat. Sci Adv 8, eadd3914 (2022). 10.1126/sciadv.add3914 [PubMed: 36269825]
63. Verbeke EJ, Mallam AL, Drew K, Marcotte EM & Taylor DW Classification of Single Particles from Human Cell Extract Reveals Distinct Structures. Cell reports 24, 259–268.e253 (2018). 10.1016/j.celrep.2018.06.022 [PubMed: 29972786]
64. Kastritis PL et al. Capturing protein communities by structural proteomics in a thermophilic eukaryote. Mol Syst Biol 13, 936 (2017). 10.15252/msb.20167412 [PubMed: 28743795]
65. Ho C-M et al. Native structure of the RhopH complex, a key determinant of malaria parasite nutrient acquisition. Proceedings of the National Academy of Sciences 118, e2100514118 (2021). 10.1073/pnas.2100514118
66. Su C-C et al. A ‘Build and Retrieve’ methodology to simultaneously solve cryo-EM structures of membrane proteins. Nature Methods 18, 69–75 (2021). 10.1038/s41592-020-01021-2 [PubMed: 33408407]
67. Danev R & Baumeister W Expanding the boundaries of cryo-EM with phase plates. Curr. Opin. Struct. Biol 46, 87–94 (2017). 10.1016/j.sbi.2017.06.006 [PubMed: 28675816]
*68. Schwartz O et al. Laser phase plate for transmission electron microscopy. Nature Methods 16, 1016–1020 (2019). 10.1038/s41592-019-0552-2 [PubMed: 31562475] This study represent an excitting hardware development with impact in applicability and interpretability of both cryo-EM and cryo-ET by dramatically improving the contrast of the images and eliminating the requirement for large defocus.

69. Jijumon AS et al. Lysate-based pipeline to characterize microtubule-associated proteins uncovers unique microtubule behaviours. Nat Cell Biol 24, 253–267 (2022). 10.1038/s41556-021-00825-4 [PubMed: 35102268]
70. Yi X, Verbeke EJ, Chang Y, Dickinson DJ & Taylor DW Electron microscopy snapshots of single particles from single cells. The Journal of Biological Chemistry 294, 1602–1608 (2019). 10.1074/jbc.RA118.006686 [PubMed: 30541924]
71. Studer D, Graber W, Al-Amoudi A & Eggli P A new approach for cryofixation by high-pressure freezing. J. Microsc 203, 285–294 (2001). https://doi.org/DOI 10.1046/j.1365-2818.2001.00919.x [PubMed: 11555146]
72. Kuba J et al. Advanced cryo-tomography workflow developments - correlative microscopy, milling automation and cryo-lift-out. J Microsc 281, 112–124 (2021). 10.1111/jmi.12939 [PubMed: 32557536]
73. Engel L et al. Lattice micropatterning for cryo-electron tomography studies of cell-cell contacts. J. Struct. Biol 213, 107791 (2021). 10.1016/j.jsb.2021.107791 [PubMed: 34520869]
74. Toro-Nahuelpan M et al. Tailoring cryo-electron microscopy grids by photo-micropatterning for in-cell structural studies. Nature Methods 17, 50–54 (2020). 10.1038/s41592-019-0630-5 [PubMed: 31740821]
75. Gorelick S et al. PIE-scope, integrated cryo-correlative light and FIB/SEM microscopy. eLife 8 (2019). 10.7554/eLife.45919
76. Boltje DB et al. A cryogenic, coincident fluorescence, electron, and ion beam microscope. eLife 11 (2022). 10.7554/eLife.82891
77. Smeets M et al. Correlative Cryo-FIB Milling using METEOR, an Integrated Fluorescent Light Microscope. Microscopy and Microanalysis 28, 1310–1310 (2022). 10.1017/S1431927622005384
78. Li W et al. Integrated multimodality microscope for accurate and efficient target-guided cryo-lamellae preparation. Nat Methods 20, 268–275 (2023). 10.1038/s41592-022-01749-z [PubMed: 36646896]
79. Klumpe S et al. A modular platform for automated cryo-FIB workflows. eLife 10 (2021). 10.7554/eLife.70506
80. Dutka M & Prokhodtseva A AutoTEM 5 – Fully Automated TEM Sample Preparation for Materials Science. Microscopy and Microanalysis 25, 554–555 (2019). 10.1017/S1431927619003507 [PubMed: 30867084]
81. Eisenstein F, Danev R & Pilhofer M Improved applicability and robustness of fast cryo-electron tomography data acquisition. J. Struct. Biol 208, 107–114 (2019). 10.1016/j.jsb.2019.08.006 [PubMed: 31425790]
82. Eisenstein F et al. Parallel cryo electron tomography on in situ lamellae. Nature Methods 20, 131–138 (2023). 10.1038/s41592-022-01690-1 [PubMed: 36456783]
83. Khavnekar S et al. Multishot tomography for high-resolution in situ subtomogram averaging. J. Struct. Biol 215, 107911 (2023). 10.1016/j.jsb.2022.107911 [PubMed: 36343843]
84. Krull A, Buchholz T-O & Jug F Noise2Void - Learning Denoising from Single Noisy Images. arXiv:1811.10980 [cs] (2019).
85. Lehtinen J et al. Noise2Noise: Learning Image Restoration without Clean Data. arXiv:1803.04189 [cs, stat] (2018).
86. Liu Y-T et al. Isotropic reconstruction for electron tomography with deep learning. Nature communications 13, 6482 (2022). 10.1038/s41467-022-33957-8
*87. Böhm J et al. Toward detecting and identifying macromolecules in a cellular context: Template matching applied to electron tomograms. Proceedings of the National Academy of Sciences 97, 14245–14250 (2000). 10.1073/pnas.230282097 This study is a beautiful example of the combination of single particle cryo-EM and cryo-ET in the structural chgaracterization of a complex biological assembly.
88. de Teresa-Trueba I et al. Convolutional networks for supervised mining of molecular patterns within cellular context. Nature Methods 20, 284–294 (2023). 10.1038/s41592-022-01746-2 [PubMed: 36690741]

89. Moebel E et al. Deep learning improves macromolecule identification in 3D cellular cryo-electron tomograms. Nature Methods 18, 1386–1394 (2021). 10.1038/s41592-021-01275-4 [PubMed: 34675434]
90. Rice G et al. TomoTwin: generalized 3D localization of macromolecules in cryo-electron tomograms with structural data mining. Nat Methods 20, 871–880 (2023). 10.1038/s41592-023-01878-z [PubMed: 37188953]
91. Arnold J et al. Site-Specific Cryo-focused Ion Beam Sample Preparation Guided by 3D Correlative Microscopy. Biophys. J 110, 860–869 (2016). 10.1016/j.bpj.2015.10.053 [PubMed: 26769364]
92. Ganeva I & Kukulski W Membrane Architecture in the Spotlight of Correlative Microscopy. Trends Cell Biol 30, 577–587 (2020). 10.1016/j.tcb.2020.04.003 [PubMed: 32402740]
93. Kukulski W et al. Correlated fluorescence and 3D electron microscopy with high sensitivity and spatial precision. J. Cell Biol 192, 111–119 (2011). 10.1083/jcb.201009037 [PubMed: 21200030]
94. Sartori A et al. Correlative microscopy: Bridging the gap between fluorescence light microscopy and cryo-electron tomography. J. Struct. Biol 160, 135–145 (2007). https://doi.org/DOI 10.1016/j.jsb.2007.07.011 [PubMed: 17884579]
95. Dahlberg PD & Moerner WE Cryogenic Super-Resolution Fluorescence and Electron Microscopy Correlated at the Nanoscale. Annu. Rev. Phys. Chem 72, 253–278 (2021). 10.1146/annurev-physchem-090319-051546 [PubMed: 33441030]
96. Dahlberg PD et al. Cryogenic single-molecule fluorescence annotations for electron tomography reveal in situ organization of key proteins in Caulobacter. Proceedings of the National Academy of Sciences 117, 13937–13944 (2020). 10.1073/pnas.2001849117
97. Tuijtel MW, Koster AJ, Jakobs S, Faas FGA & Sharp TH Correlative cryo super-resolution light and electron microscopy on mammalian cells using fluorescent proteins. Sci Rep 9, 1369 (2019). 10.1038/s41598-018-37728-8 [PubMed: 30718653]
98. Wang Q, Mercogliano CP & Löwe J A Ferritin-Based Label for Cellular Electron Cryotomography. Structure 19, 147–154 (2011). 10.1016/j.str.2010.12.002 [PubMed: 21300284]
99. Silvester E et al. DNA origami signposts for identifying proteins on cell membranes by electron cryotomography. Cell 184, 1110–1121.e1116 (2021). 10.1016/j.cell.2021.01.033 [PubMed: 33606980]
100. Fung HKH et al. Genetically encoded multimeric tags for subcellular protein localization in cryo-EM. Nat Methods 20, 1900–1908 (2023). 10.1038/s41592-023-02053-0 [PubMed: 37932397]
101. Schorb M, Haberbosch I, Hagen WJH, Schwab Y & Mastronarde DN Software tools for automated transmission electron microscopy. Nat Methods 16, 471–477 (2019). 10.1038/s41592-019-0396-9 [PubMed: 31086343]
102. Lucas BA & Grigorieff N Quantification of gallium cryo-FIB milling damage in biological lamellae. Proc Natl Acad Sci U S A 120, e2301852120 (2023). 10.1073/pnas.2301852120 [PubMed: 37216561]
103. Berger C et al. Plasma FIB milling for the determination of structures in situ. Nature communications 14, 629 (2023). 10.1038/s41467-023-36372-9
104. Laughlin TG et al. Architecture and self-assembly of the jumbo bacteriophage nuclear shell. Nature 608, 429–435 (2022). 10.1038/s41586-022-05013-4 [PubMed: 35922510]
105. Lacey SE, Foster HE & Pigino G The molecular structure of IFT-A and IFT-B in anterograde intraflagellar transport trains. Nature Structural & Molecular Biology 30, 584–593 (2023). 10.1038/s41594-022-00905-5
106. Wozny MR et al. In situ architecture of the ER–mitochondria encounter structure. Nature, 1–5 (2023). 10.1038/s41586-023-06050-3
107. Baek M et al. Accurate prediction of protein structures and interactions using a three-track neural network. Science (New York, N.Y.) 373, 871–876 (2021). 10.1126/science.abj8754 [PubMed: 34282049]
108. Jumper J et al. Highly accurate protein structure prediction with AlphaFold. Nature 596, 583–589 (2021). 10.1038/s41586-021-03819-2 [PubMed: 34265844]
109. Graziadei A & Rappsilber J Leveraging crosslinking mass spectrometry in structural and cell biology. Structure 30, 37–54 (2022). 10.1016/j.str.2021.11.007 [PubMed: 34895473]

*110. O'Reilly FJ et al. In-cell architecture of an actively transcribing-translating expressome. Science (New York, N.Y.) 369, 554–557 (2020). 10.1126/science.abb3758 [PubMed: 32732422] This study combined cellular cryo-ET with in-cell crosslinking and whole cell proteomics, and illustrates the power of integrative approaches to capture elusive and transient complexes.

111. Lucas BA et al. Locating macromolecular assemblies in cells by 2D template matching with cisTEM. eLife 10, e68946 (2021). 10.7554/eLife.68946 [PubMed: 34114559]

112. Rickgauer JP, Grigorieff N & Denk W Single-protein detection in crowded molecular environments in cryo-EM images. eLife 6 (2017). 10.7554/eLife.25648

113. Lucas BA, Himes BA & Grigorieff N Baited reconstruction with 2D template matching for high-resolution structure determination in vitro and in vivo without template bias. eLife 12 (2023). 10.7554/eLife.90486

114. Narayan K & Subramaniam S Focused ion beams in biology. Nature Methods 12, 1021–1031 (2015). 10.1038/nmeth.3623 [PubMed: 26513553]

115. Xu CS et al. An open-access volume electron microscopy atlas of whole cells and tissues. Nature 599, 147–151 (2021). 10.1038/s41586-021-03992-4 [PubMed: 34616045]

116. Smith D & Starborg T Serial block face scanning electron microscopy in cell biology: Applications and technology. Tissue Cell 57, 111–122 (2019). 10.1016/j.tice.2018.08.011 [PubMed: 30220487]

117. Harkiolaki M et al. Cryo-soft X-ray tomography: using soft X-rays to explore the ultrastructure of whole cells. Emerging Topics in Life Sciences 2, 81–92 (2018). 10.1042/ETLS20170086 [PubMed: 33525785]

118. Mahamid J et al. Visualizing the molecular sociology at the HeLa cell nuclear periphery. Science (New York, N.Y.) 351, 969–972 (2016). 10.1126/science.aad8857 [PubMed: 26917770]

119. Kasinath V et al. JARID2 and AEBP2 regulate PRC2 in the presence of H2AK119ub1 and other histone modifications. Science 371 (2021). 10.1126/science.abc3393

*120. Mosalaganti S et al. AI-based structure prediction empowers integrative structural analysis of human nuclear pores. Science 376, eabm9506 (2022). 10.1126/science.abm9506 [PubMed: 35679397] This study capatilized on AlphaFold2 and cryo-ET data for structural modeling of the human nuclear pore complex with unprecedented precision and completeness.

121. Gemmer M et al. Visualization of translation and protein biogenesis at the ER membrane. Nature 614, 160–167 (2023). 10.1038/s41586-022-05638-5 [PubMed: 36697828]

122. Hoffmann PC et al. Tricalbins Contribute to Cellular Lipid Flux and Form Curved ER-PM Contacts that Are Bridged by Rod-Shaped Structures. Dev Cell 51, 488–502.e488 (2019). 10.1016/j.devcel.2019.09.019 [PubMed: 31743663]

123. Lucas BA, Zhang K, Loerch S & Grigorieff N In situ single particle classification reveals distinct 60S maturation intermediates in cells. eLife 11 (2022). 10.7554/eLife.79272

124. De Rosier DJ & Klug A Reconstruction of Three Dimensional Structures from Electron Micrographs. Nature 217, 130–134 (1968). 10.1038/217130a0 [PubMed: 23610788]

125. Dubochet J & McDowall AW Vitrification of pure water for electron microscopy. J. Microsc 124, RP3–RP4 (1981). 10.1111/j.1365-2818.1981.tb02483.x

126. Frank J Averaging of low exposure electron micrographs of non-periodic objects. Ultramicroscopy 1, 159–162 (1975). [PubMed: 1236029]

127. Hart RG Electron microscopy of unstained biological material: the polytropic montage. Science 159, 1464–1467 (1968). [PubMed: 4183952]

128. Cheng Y, Grigorieff N, Penczek PA & Walz T A primer to single-particle cryo-electron microscopy. Cell 161, 438–449 (2015). 10.1016/j.cell.2015.03.050 [PubMed: 25910204]

129. Chen Z et al. In situ cryo-electron tomography reveals the asymmetric architecture of mammalian sperm axonemes. Nature Structural & Molecular Biology 30, 360–369 (2023). 10.1038/s41594-022-00861-0

130. Hoffmann PC et al. Structures of the eukaryotic ribosome and its translational states in situ. Nature communications 13, 7435 (2022). 10.1038/s41467-022-34997-w

131. Wan W & Briggs JAG Cryo-Electron Tomography and Subtomogram Averaging. Method Enzymol 579, 329–367 (2016). 10.1016/bs.mie.2016.04.014

132. Wang Z et al. The molecular basis for sarcomere organization in vertebrate skeletal muscle. Cell 184, 2135–2150.e2113 (2021). 10.1016/j.cell.2021.02.047 [PubMed: 33765442]

133. Pyle E & Zanetti G Current data processing strategies for cryo-electron tomography and subtomogram averaging. Biochem. J 478, 1827–1845 (2021). 10.1042/BCJ20200715 [PubMed: 34003255]

134. consortium, w. Protein Data Bank: the single global archive for 3D macromolecular structure data. Nucleic Acids Res 47, D520–D528 (2018). 10.1093/nar/gky949

135. Lawson CL et al. EMDataBank unified data resource for 3DEM. Nucleic Acids Res 44, D396–D403 (2016). 10.1093/nar/gkv1126 [PubMed: 26578576]

136. Iudin A et al. EMPIAR: the Electron Microscopy Public Image Archive. Nucleic Acids Res 51, D1503–D1511 (2023). 10.1093/nar/gkac1062 [PubMed: 36440762]

Box 1:

Differences between cryo-EM and cryo-ET

While in both cryo-EM and cryo-ET the samples are imaged in a frozen-hydrated vitreous state and using a transmission electron microscope of similar if not identical configuration, there are fundamental differences between the two methodologies (for some classical references on vitrification and 3D reconstruction principles see [26,124–127]).

Most obviously, they differ on the data collection strategy used: single images (cryo-EM) versus tilt series (cryo-ET). When the object is imaged only once, the full electron dose allowed by radiation damage can be used to generate a high(er) signal-to-noise ratio, and therefore a high(er) resolution image. Typically, thousands of images are taken, each one containing between tens and hundreds of "particles" to generate datasets containing hundreds of thousands, if not millions of particle images of the biological molecule of interest. A central assumption is that the particles are sufficiently self-consistent, and that they are viewed in different orientations. Through a computational pipeline [128] that involves alignment and classification schemes, both in 2D and 3D, and a refinement that iteratively defines the relative angles of the different views being analyzed, the selected images are merged together in one or several reconstructions that, if successful, result in density maps of sufficient resolution to allow the generation of an atomic model (typically at < 4 Å resolution). However, in complex samples, like inside the cell, particles densely stacked along the projection direction will produce overlapping signal in the 2D image. Typically, instead of taking a single image of a particular area in such samples, a series of images is acquired at different tilts, and the dose is fractionated across the multiple tilt images. Thus, each image in the tilt series has a low signal-to-noise ratio, which progressively deteriorates as the sample is tilted to higher angles due to the thicker effective cross section that the beam must go through. Using a pipeline that involves alignment of the tilt images in 2D, followed by 3D reconstruction, a tomographic volume is generated with improved signal-to-noise ratio and contrast than the individual images. This 3D volume, or tomogram, contains a somewhat distorted representation of the macromolecular 3D structures; although the original images are typically collected at 1–4 Å per pixel, tomograms only show resolvable details in the 2–5 nm range. This deteriorated resolution originates from technical limitations of tilting the stage inside the electron microscope and the restricting sample grid geometry, leading to incomplete sampling ("missing wedge"), and from the substantial non-linear deformation and damage that the biological material experiences when bombarded with the large number of electrons required to generate a tilt-series (in the range of 120 $e^{-}/Å^{2}$). These limiting factors can be mitigated by the generation of subtomogram averages when self-consistent structures viewed in different orientations exist in the 3D tomograms, a process that involves alignment, classification and merging of the selected particles into reconstructions similarly to how it is done in single particle cryo-EM. This practice has started to yield resolutions better than 7 Å [41,42,121,129–133].

Box 2 -

Cryo-EM and cryo-ET data accessibility

Many years ago, the maturity of the X-ray crystallography field both allowed and demanded that the coordinates of structural models be deposited following publication, so that the entire scientific community could mine the richness of information contained in such structures. The PDB [134] was born to host X-ray, NMR and the rare electron crystallography structure. As the single particle cryo-EM field gained output and maturity, the same became a requirement of its structures and maps (the latter deposited in the EMDB [135]). Image analysis developers have benefited from availability of raw data which, in the case of EM, is deposited in EMPIAR [136]. The discussion on whether and how to make available tomographic data is still open. It is absolutely clear that it would help to speed up technical developments and to increase the biological insight mined from each tomogram, thus propelling the advancement of cryo-ET as an emerging method in structural biology. But it is also clear that the community needs careful thought about cryo-ET data deposition that maintains meaningful connectivity across the significantly different data types, from the raw micrographs in a large number of tilt-series, through reconstructed 3D volumes, coordinates of localized particles, annotations of their identified functional states, and their mapping into the original volume in the form of 3D segmentations. It is important to also consider that the latter data types would be of interest to researchers in different disciplines, like cell biologists, who may not be familiar with file formats specific to the cryo-EM field. Therefore, for these data to be helpful, specially to those without a structural biology background, it is important to implement user friendly visualization of the tomograms and segmentations, and to facilitate retrieval of quantified and localized particle data, which can describe, for example, the molecular concentrations of functional complexes and their distribution across different subcellular areas or cell states.

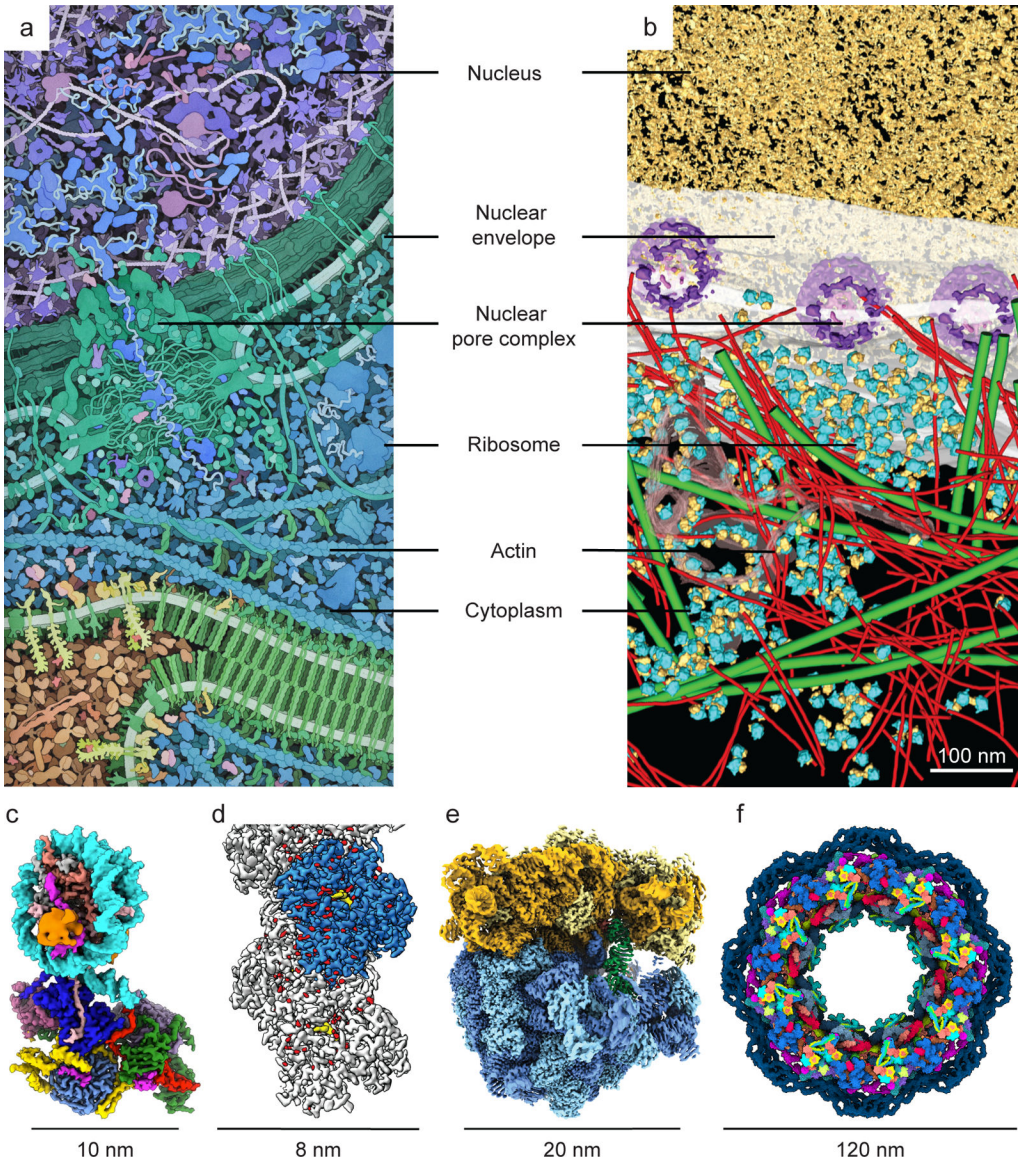

Figure 1. Realization of a structural biologist's dream

A. Illustration by David S. Goodsell depicts the VegF signaling pathway. Blood serum is at bottom left. Cell membranes are shown in green, with VegF receptor in yellow green and a disassembling adherent junction in darker green at the bottom. Multiple kinases (pink) are activated and travel through the cytoplasm (blue) and the nuclear pore (green, at center) to phosphorylate transcription factors in the nucleus (purple). Adapted from [3]. **B.** Annotated rendering of cryo-ET data depicting a HeLa cell nuclear periphery. The nuclear envelope (transparent white) with nuclear pore complexes (purple) separates the nucleus (gold) from the cytoplasm containing ribosomes (blue and yellow), microtubules (green) and actin (red). Adapted from [118]. **C-E.** High resolution reconstructions of macromolecular assemblies visualized *in vitro* by cryo-EM: **C.** Human Polycom Repressive Complex 2 (PRC2) at ~3.5 Å resolution interacting with a nucleosomal substrate (DNA shown in cyan) recognizing a ubiquitin in histone H2A (orange) as the SET domain of EZH2 (blue) engages

the histone H3 tail (pink) for methylation. Other domains of EZH2 are shown in yellow and maroon, EED in light blue, SUZ12 in green, RBAP48 in grey, AEBP2 in red, and JARID2 in magenta. From [119]. **D.** Actin filaments in the Mg2+-ADP-BeF_3- state at ~2.2 Å resolution. One actin subunit is coloured blue, the nucleotide is yellow, and ordered waters red. Adapted from [21]. **E.** Bacterial translating ribosome at 1.55 Å resolution coloured in dark yellow (16S rRNA), light yellow (ribosomal proteins in the small subunit), light blue (large subunit ribosomal proteins), dark blue (23S and 5S rRNA). Adapted from [14]. **F.** A structural model of the human nuclear pore complex built using integrative structural modelling with AlphaFold2 and a density map from cryo-ET of isolated nuclei. Adapted from [120].

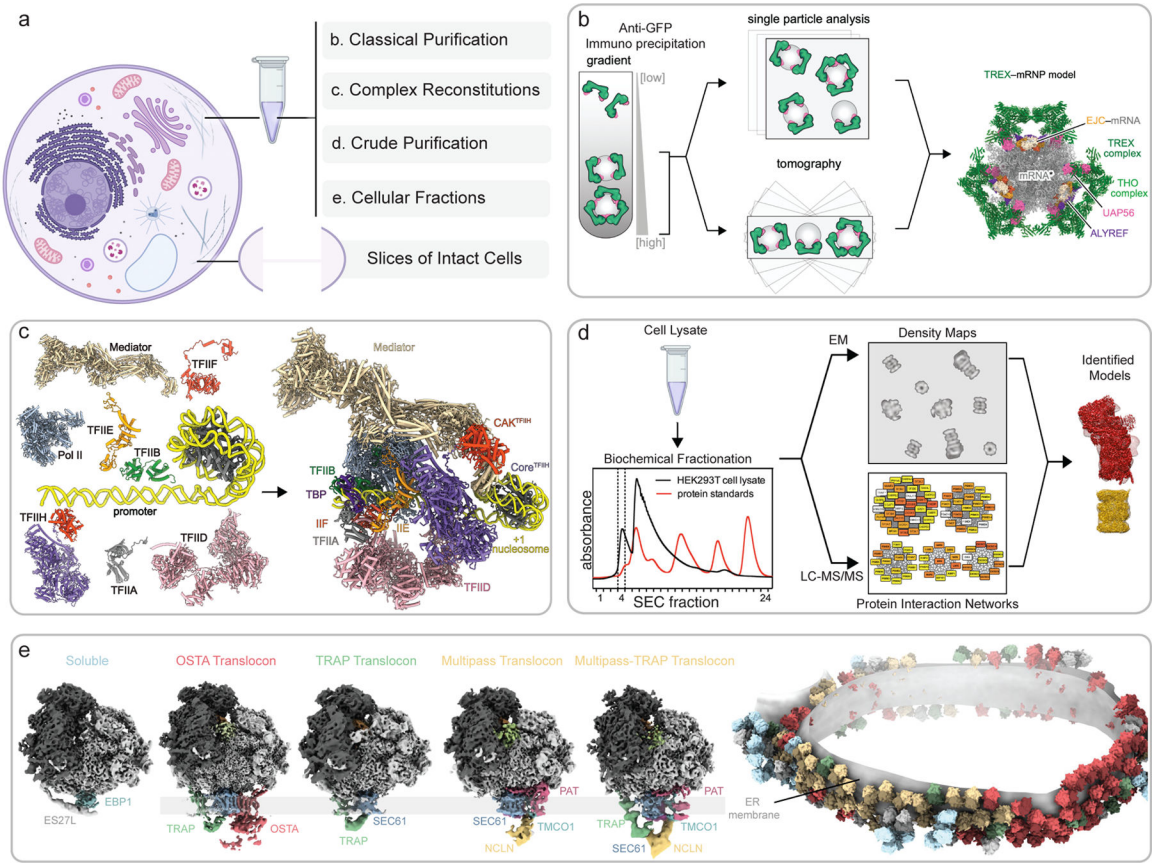

Figure 2. Increasing sample complexity by a continuum of cryo-EM methods

A. Overview of the spectrum of samples for cryo-EM/ET. **B.** Pulldown on a GFP-tagged subunit of the TREX complex directly from a nuclear extract followed by sucrose gradient fractionation provide samples for both high-resolution single particle cryo-EM and cryo-ET of RNPs, leading to the determination of a pleomorphic mRNA core bounded by structurally-defined TREX complexes necessary for nuclear export of RNPs. Adapted from [60]. **C.** *In vitro* reconstitution of the PIC-mediator supracomplex on chromatinized core promoter DNA from individual complexes (left) allowed cryo-EM analysis that led to a structural model for the full functional assembly (right)[12]. **D.** Pipeline for structural analysis of heterogeneous mixtures of human cell lysates, combining shotgun cryo-EM analysis and classification with protein identification by mass spectrometry. Adapted from [63]. **E.** Complex ribosomal assemblies engaged with the integral-membrane translocon studied by cryo-ET of microsomal fractions from human cells (right). The protein-conducting channel SEC61 associates with distinct combinations of cofactors, such as TRAP and OSTA (left), reflecting the requirements of different protein substrates in cells. Adapted from [121].

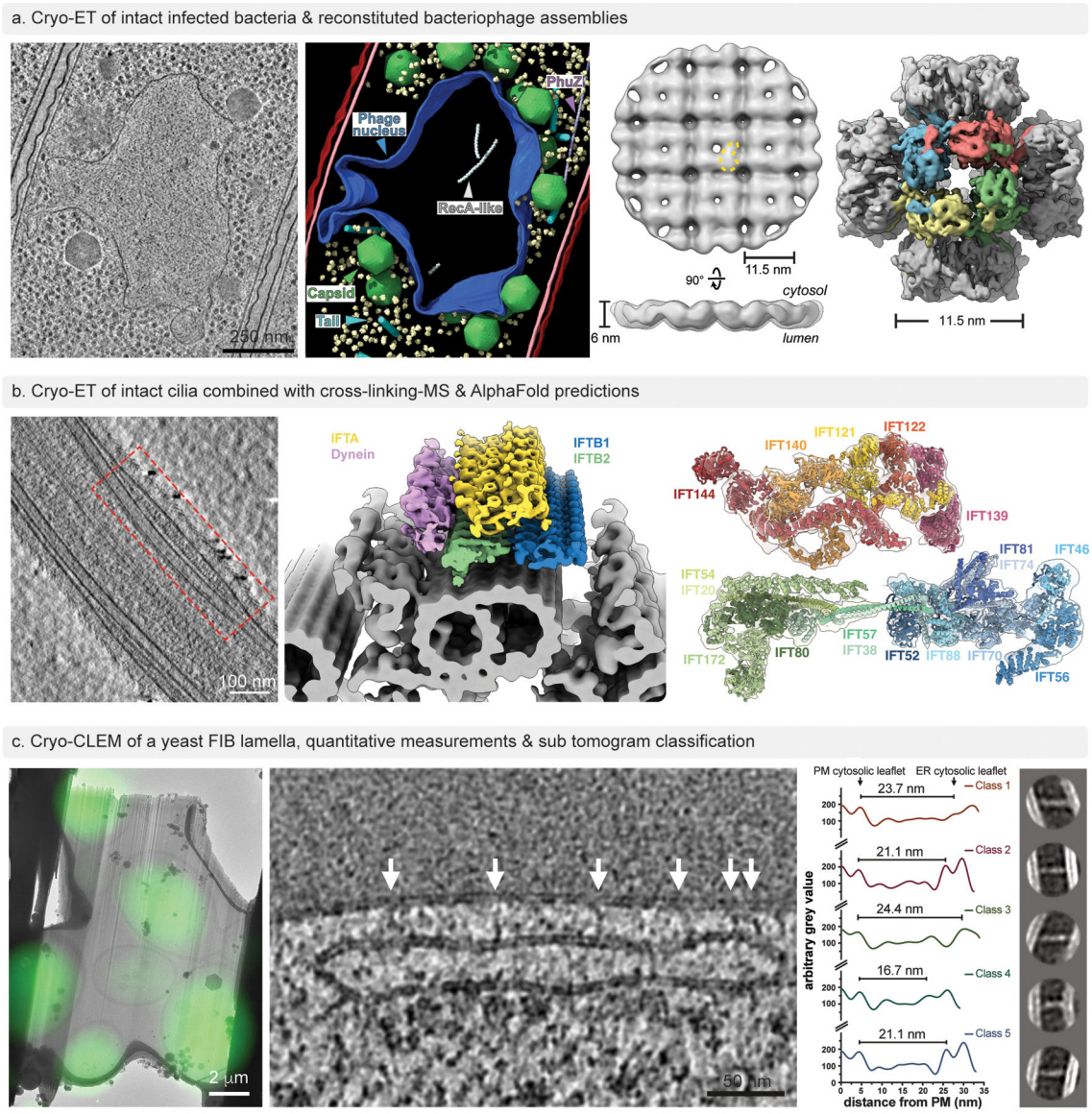

Figure 3. Cryo-ET visualizes complex cell biology.

A. Cryo-ET study of bacteriophage-infected cells. The phage assembles a nuclear shell from one protein (chimallinA). From left to right: tomographic slice; segmented cryo-tomogram; subtomogram average of the phage "nucleus" and structure resolved by cryo-ET of a minimal chimallin shell reconstituted *in vitro*. Adapted from [104]. **B.** Cryo-ET of intact *Chlamydomonas reinhardtii* cilia revealing the intraflagellar transport machinery or trains (IFT). From left to right: tomographic slice; a composite map obtained from subtomograms averaging of four IFT components showing the independently refined domains of the anterograde trains positioned above the microtubule doublet (grey), with IFTB1 (blue), IFTB2 (green), dynein (pink), and IFTA (yellow); structural model of IFTA and IFTB derived from Alphafold2 and fitted into the cryo-ET density using molecular dynamics flexible fitting. Adapted from [105]. **C.** Cryo-ET study of contacts between the endoplasmic reticulum (ER) and plasma membrane (PM) in budding yeast. From left to right: overlay of

cryo-fluorescence microscopy image (GFP channel, acquired before FIB milling) and cryo-EM image of a lamellae of budding yeast cells expressing GCaMP, a fluorescent indicator of intracellular Ca2+ concentration; tomographic slice showing ER-PM contacts (arrows) in a budding yeast cell overexpressing Tcb3-EGFP; density projection profiles along the major axis of the bridges seen in the 2D class averages (right most) obtained by subtomogram averaging of the bridge structures. For each profile, the indicated length measured between the cytosolic leaflets of the PM and the ER provides an estimate of the length of the different bridge classes. Adapted from [122].

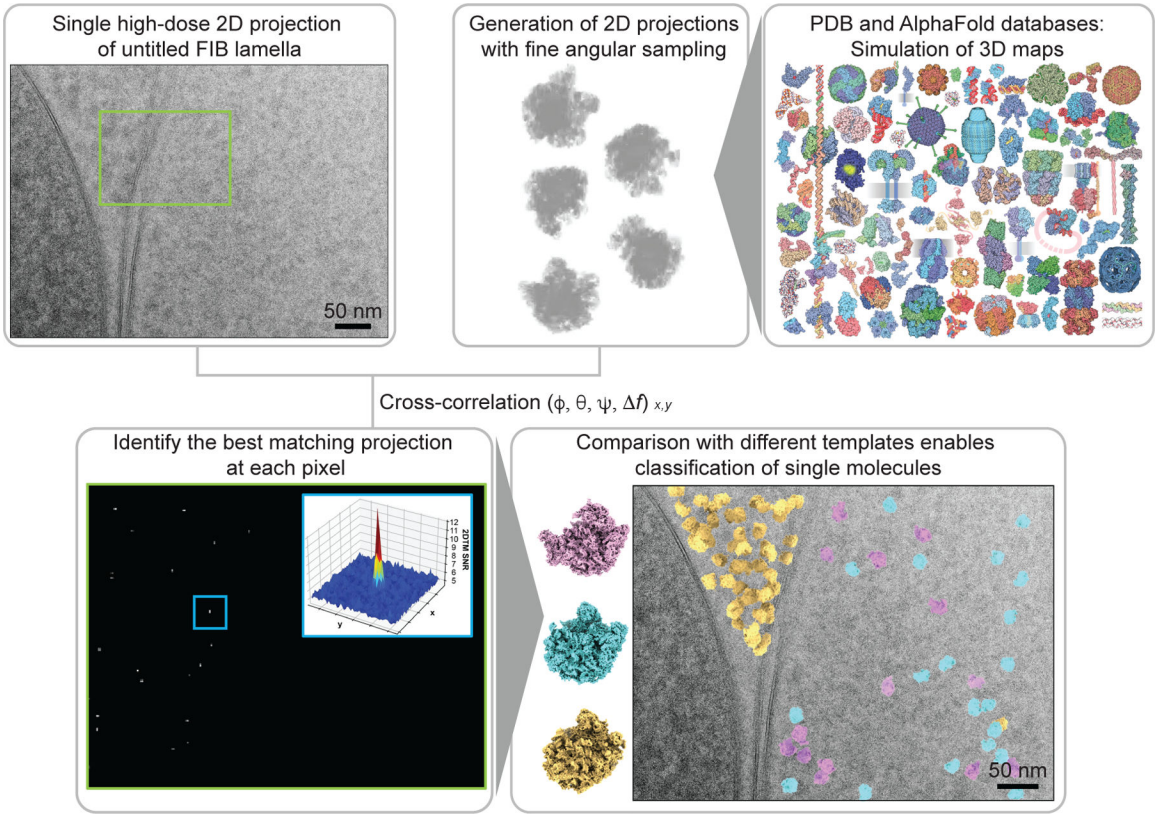

Figure 4. In situ cryo-EM with 2D template matching.

Pipeline for the use of 2D template matching: high-dose, high-resolution 2D projection images of a cellular slice (from FIB milling, top left), are matched against (a number of) available high-resolution structures from structural databases or structure prediction (top right); high correlations scores indicate the presence of the template in the cellular volume (bottom left), allowing to position the identified structures in the cellular context (bottom right). Adapted from [123].